DIPSI Workshop 2011 on Droplet Impact Phenomena & Spray Investigation
May 27, 2011, Bergamo, Italy

DROP IMPACT OF A CONCENTRATED COLLOIDAL SUSPENSION

M. Muratore[1], V. Bertola[1], M.D. Haw[2]

[1]University of Liverpool, School of Engineering, Harrison Hughes Building, Liverpool L69 3BX, UK
[2]University of Strathclyde, Department of Chemical and Process Engineering, James Weir Building, 75 Montrose Street, Glasgow G1 1XJ, UK

ABSTRACT
The impact of drops of a concentrated colloidal suspension of nearly hard-core particles in octadecene (volume fraction: 59.6%) onto solid surfaces is studied experimentally by high-speed imaging, for impact Weber numbers ranging between 26 and 262, and for different values of the target surface energy. Upon impact, these drops do not exhibit inertial spreading, which is observed for other Newtonian and non-Newtonian fluid drops. On wettable surfaces (glass), impact is followed by capillary-driven spreading at the same rate observed in Newtonian fluids (Tanner's law), while on less wettable surfaces (PTFE) colloidal suspension drops relax to achieve the shape of a spherical cap, but do not spread. This peculiar impact morphology, and in particular the absence of inertial spreading, is interpreted as a consequence of dilatancy and jamming occurring upon impact.

INTRODUCTION

The impact morphology of liquid droplets onto solid, dry surfaces, is well-known (see e.g. [1-4]). Upon impact, the liquid spreads on the surface taking the form of a disk; for low impact velocity, the disk thickness is approximately uniform, while for higher impact velocities the disk is composed of a thin central part (often called "lamella") surrounded by a circular rim. This initial spreading stage is typically very fast (≈5 ms). After the drop has reached maximum spreading, two qualitatively different outcomes are possible.

If the initial kinetic energy exceeds a threshold value capillary forces are insufficient to maintain the integrity of the drop, which disintegrates into smaller satellite droplets jetting out of its outermost perimeter (splashing). If splashing does not occur, the drop is allowed to retract under the action of capillary forces, which tend to minimize the contact with the surface; in some cases, retraction is so fast that the liquid rises in the middle forming a Worthington jet, which may subsequently result in the complete rebound of the drop from the surface.

Whilst there exists a significant volume of literature about single drop impacts of simple (Newtonian) fluids, the number of works about fluids with complex microstructure (polymer melts or solutions, gels, pastes, foams and emulsions, etc.) is comparatively very small. However, these fluids are frequently used in common applications, such as painting, food processing, and many others.

The microscopic structure of fluids is described from the macroscopic point of view of continuum mechanics by constitutive equations, which express the relationship between the stress tensor and the velocity gradient. Simple liquids, such as water, are generally characterized by a Newtonian constitutive equation, where the stress tensor is a linear function of the velocity gradient, whereas in complex (or non-Newtonian) fluids the stress tensor is a generic function of the velocity gradient and of its derivatives. [5,6].

Thus, the study of non-Newtonian drops requires a completely different modelling approach, as well as different sets of experimental data, depending on the form of the constitutive equation of the fluid. In particular, due to the large spatial and temporal gradients observed during drop impacts, small changes in the constitutive equation result into large macroscopic effects (for example, most drop impact models become inaccurate for large fluid viscosities [7]).

An important example of complex fluid is represented by pastes, which are widely used in many industrial processes such as cosmetics, pharmaceutical, and food industry. Pastes can be described as concentrated suspensions of colloidal particles (i.e., particles with size in the range between a few nm and a few μm) in a fluid medium.

Despite the practical importance of colloidal flows [8,9], they are still poorly understood in comparison with other complex fluids, and studies on model systems were carried out only recently [10]. A peculiar characteristic of colloidal flows is the appearance of strong non-linearities, such as yielding, shear-thickening, and shear localisation or apparent wall slip due to particle depletion near solid walls [11-14]. Moreover, specific applications (e.g., microfluidics) may involve geometric dimensions comparable with the particle size, leading to confinement effects [15].

When a highly concentrated suspension of particles is forced to flow, its volume must increase on shearing to enable motion. Dilation within a fixed volume of suspending liquid eventually causes particles to encounter the air-liquid interface. This generates large capillary forces at the free surface, which can then balance the normal inter-particle forces and resist further motion, jamming the sample [16].

This work presents the preliminary results of drop impact experiments of a suspension of near hard-core colloidal particles, with the purpose to investigate the impact morphology in the presence of shear thickening or jamming, which may be induced by the large velocity gradients arising upon drop impact.

MATERIALS AND METHODS

Fluid preparation and characterisation

A model colloidal suspension characterised by nearly hard-core (purely repulsive) interactions was prepared with poly-methyl-methacrylate (PMMA, density: 1180 kg/m^3) spheres (radius r ~ 604nm, 5% polydispersity) sterically stabilised by poly-12-hydroxy stearic acid (PHSA) chemically grafted onto their surface [17], and suspended in octadecene (density: 789 kg/m^3; surface tension: 0.03 N/m).

In order to ensure that particles interact as hard spheres, the fluid medium must be a poor solvent for PMMA, in order to limit particles swelling, but a good solvent for PHSA so that polymer chains stretch out. When two particles come into contact, the repulsive energy given by the superposition of the two polymer layers rapidly increases as the distance between particles reduces [18]. Among the various suitable solvents, octadecene was selected because of its very low volatility.

Suspensions were centrifuged at 2000 rpm for 12 hours to create a sediment, which was assumed to have a concentration of 64% (random close packing or maximum random packing) [19]. The sediment was then diluted with octadecene to a concentration of 59.6%, corresponding to a density of 1022 kg/m^3.

According to the equilibrium thermodynamics phase diagram of ideal hard-spheres [20], for volume fractions between 54.5% and 74% (maximum crystalline close packing fraction) the system is crystalline. However, experiments showed that model suspensions of sterically-stabilized colloidal hard-spheres failed to crystallize for volume fractions greater than 58%, remaining in a non-equilibrium phase known as the colloidal glass [21].

Figure 1 shows examples of flow curves for dense hard-sphere suspensions at different volume fractions [22]. For concentrations above 56%, fluids exhibit strong shear thickening at shear rates of the order of 50 s^{-1}.

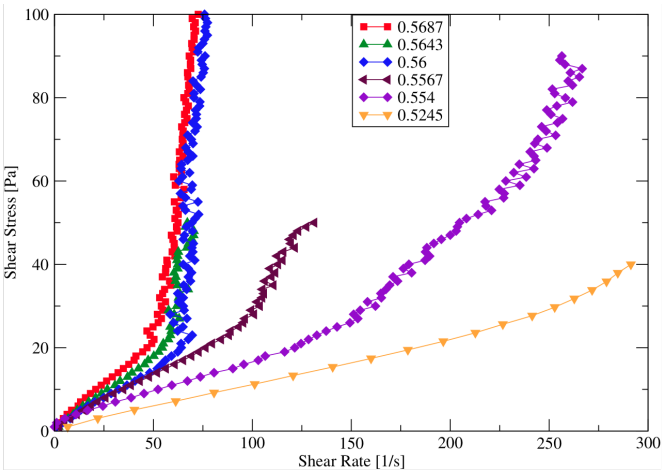

Figure 1. Flow curves of dense suspensions of PMMA particles (r = 613 nm), for different volume fractions [22].

Shear-thickening could be an indication of jamming inside the fluid sample. Indeed, dilatancy and jamming can be directly related to shear-thickening during extensional rheology experiments [23]. For shear rates below the shear-thickening point, fluids exhibit a Newtonian behaviour, with shear viscosities of the order of 0.5 Pa·s.

For the sake of comparison, a Newtonian fluid with a measured viscosity of 0.55 Pa·s was obtained by preparing a 96% solution of glycerol in water (density: 1250 kg/m^3).

Experimental setup and procedure

Drops were generated using a syringe with blunt hypodermic needle (gauge 21, 0.495 mm i.d.) driven by a micrometric screw, and detached under their own weight. The needle was suspended above two substrates of different surface energy (glass and PTFE). To change the impact velocity, the drop release height was adjusted between 2 and 18 cm using a Vernier height gauge, which corresponds to theoretical free-fall velocities between 0.6 and 1.9 m/s.

The competition between inertia and surface forces was characterised through the Weber number, $We = \rho v^2 D_0/\sigma$, where ρ is the suspension density, σ is the solvent surface tension, v is the drop velocity, and D_0 the characteristic diameter before impact.

A high-frame rate CMOS camera (Phantom v9000) equipped with a zoom lens (Navitar 7000) and horizontally aligned with the surface recorded the impacts of single drops. Back-to-front illumination was provided by a LED backlight (Philips AccentLed) which ensured a uniform illumination intensity, and images with a resolution of 576×576 pixels were captured at 4000 frames per second. Magnification was kept constant throughout all experiments and lengths on the image could be calculated by comparison with a reference length (spatial resolution: 16.26 μm/pixel). To ensure a fine optical alignment, the camera, the heated surface and the backlight were fixed to an optical breadboard.

Quantitative data were extracted from images using proprietary software developed in LabView environment, which after background subtraction and image optimization measured the base diameter of drops, as well as the left and right contact angles using the drop profile tangent method.

The characteristic drop diameter before impact, measured by comparison with a known reference length, was 2.208±0.075 mm, resulting into Weber numbers ranging from 26 to 262.

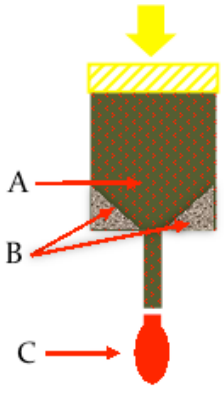

Figure 2. Schematic of the syringe-needle dispensing system (see text for description).

Although the syringe-needle dispensing system described above ensures a very good reproducibility of the drop diameter, the particle concentration may not remain constant as the two-phase (solid-liquid) mixture is pushed through the needle. In fact, the higher resistance encountered in the sudden contraction and in the needle is likely to induce self-filtration, favouring the flow of the suspending liquid with respect to particles. With reference to Figure 2, when the mixture approaches the contraction (a) the velocity of particles becomes smaller than that of the liquid (i.e., the liquid/solid slip ratio become greater than one); some of the particles accumulate in the corners of the contraction (b). Thus, the particle concentration in the drop (c) is probably smaller than in the syringe reservoir, and slowly varies as the syringe is emptied.

RESULTS

Figure 3 compares the drop impact morphologies of colloidal drops impacting with the same Weber number (We=145) on solid substrates characterised by different surface energy (glass and PTFE).

These images suggests that at the moment of impact colloidal suspension drops are not necessarily spherical, but may exhibit deformations created at the moment of drop generation, similar to what happens during the generation of viscoplastic drops from capillary nozzles [24]. Such deformations eventually disappear as the drop is deposited on the target surface and takes the shape of a spherical cap under the action of capillary forces. These images also show that the inertial spreading of drops, which usually occurs in the first 5 ms after impact, is not noticeable on either surface, although one can observe capillary-driven spreading on the glass substrate at longer times after the impact.

The base diameter (non-dimensionalised with respect to the characteristic drop diameter, D_0) of colloidal suspension drops impacting on a glass surface is plotted as a function of time in Figure 4, for different impact velocities hence different Weber numbers. Upon impact, the drop base diameter has a modest inertial deformation for less than 1 ms, then remains almost constant before the beginning of capillary-driven spreading. Surprisingly, increasing the Weber number, i.e. the impact kinetic energy, reduces the inertial deformation; moreover, in the range of Weber numbers considered, at the end of inertial expansion the base diameter remains smaller than the drop equilibrium diameter.

These observations suggest that upon impact the colloidal suspension jams, and therefore large inertial deformations are not possible; increasing the impact kinetic energy jamming is quicker, which further reduces the inertial deformation. For longer times (> 100 ms), irrespective of the Weber number, spreading continues at the rate $D \sim t^{1/10}$, as predicted by Tanner's law for Newtonian drops [25].

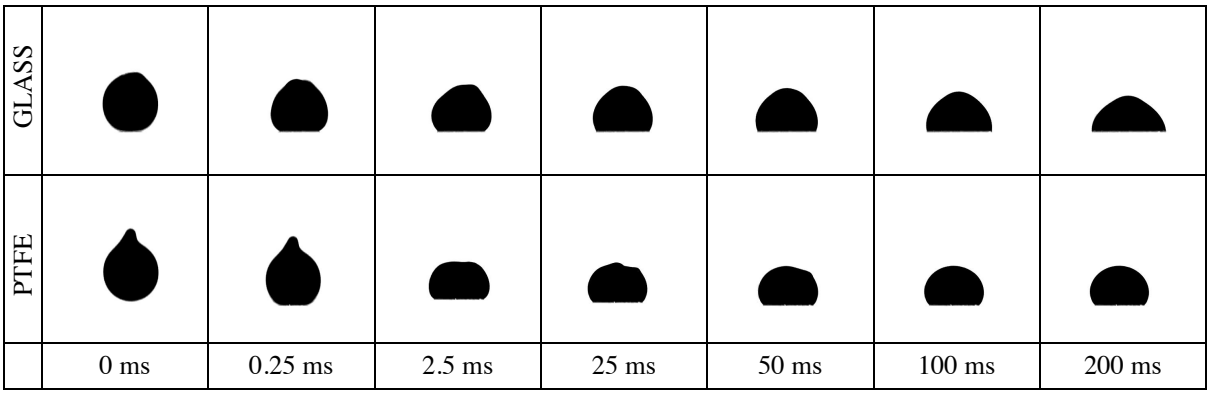

Figure 3. Drop impact morphology of colloidal suspension drops (volume fraction: 59.6%) impacting on glass and PTFE surfaces, for We = 145.

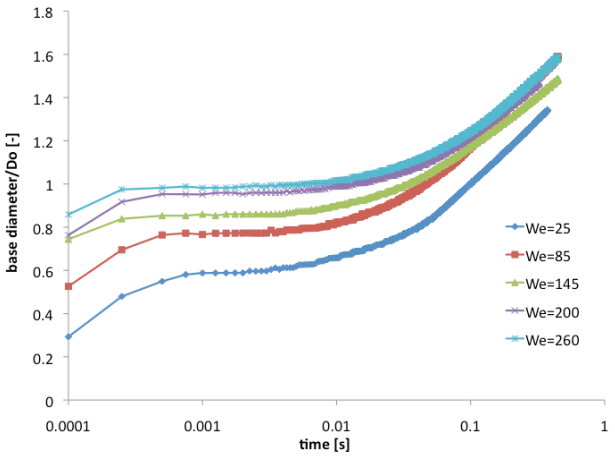

Figure 4. Dimensionless base diameter of colloidal suspension drops (Φ = 59.6%) impacting on a glass surface.

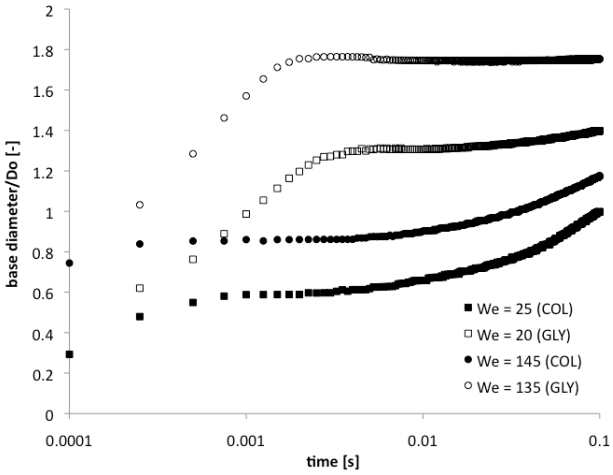

Figure 5. Comparison between the base diameters of colloidal suspension drops and Newtonian drops impacting on glass.

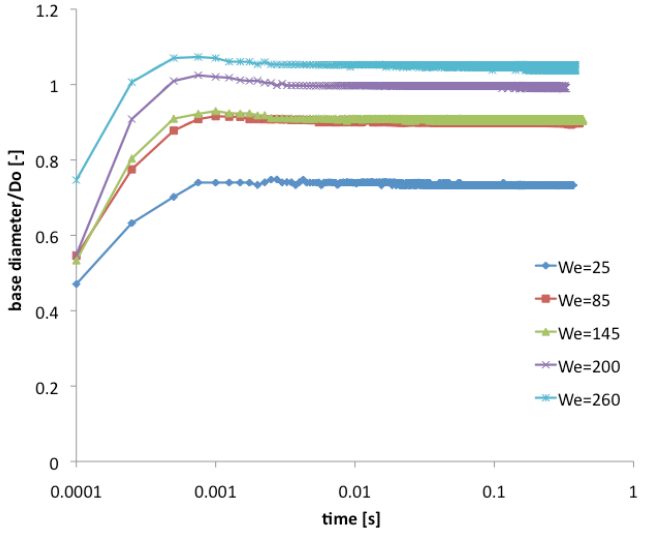

Figure 6. Dimensionless base diameter of colloidal suspension drops (Φ = 59.6%) impacting on a PTFE surface.

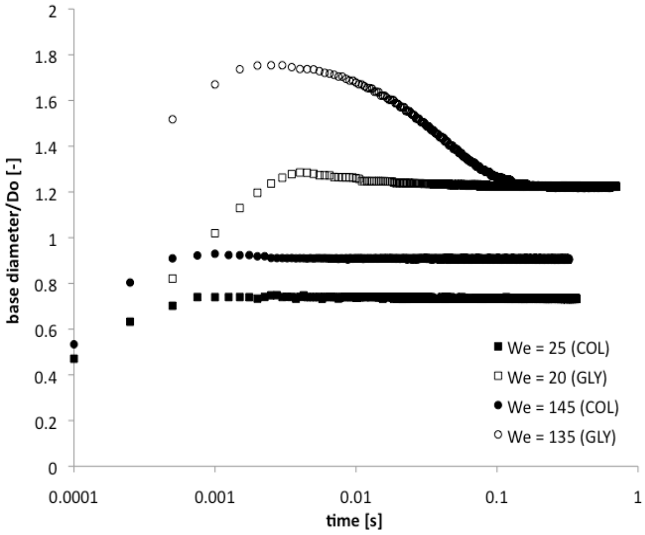

Figure 7. Comparison between the base diameters of colloidal suspension drops and Newtonian drops impacting on PTFE.

Figure 5 compares the base diameters of two colloidal suspension drops and two Newtonian drops with a viscosity of 0.55 Pa·s (i.e., a viscosity similar to that of the colloidal suspension before shear-thickening, see Figure 1). Despite the similar viscosity, the inertial spreading of the Newtonian drops is larger and has a longer duration (3-5 ms) than that of colloidal suspension drops; as expected, the drop deformation increases as the Weber number grows. This comparison provides further evidence that the impact on a solid substrate, even from a modest falling height, is able to cause jamming in colloidal suspension drops.

Figure 6 shows the base diameter of colloidal drops impacting on a PTFE surface. The inertial deformation upon impact is again of very small amplitude and short duration (about 1 ms). Unlike in the case of the glass surface, no capillary-driven spreading can be observed, and the base diameter remains constant for an indefinite time. It is interesting to observe that drops with different impact Weber numbers do not exhibit the tendency to attain a same equilibrium value of the base diameter, i.e. the value determined by the Young-Laplace equation, but seem to remain frozen (jammed) in the state they reach upon impact.

The comparison with Newtonian drops impacting on the same surface (Figure 7) shows that, in addition to significant inertial deformations, Newtonian drops are also able to partially retract, in order to attain the equilibrium base diameter value. Note that the equilibrium value of the glycerol solution drops base diameter is significantly different from any of the colloidal suspension drop base diameters because the fluids have different surface tensions. Moreover, in colloidal suspension drops the base diameter (hence the contact angle) depends strongly on the impact Weber number, meaning that the contact angle cannot be determined using the Young-Laplace equation, but rather depends on the initial small inertial deformation and on particles jamming.

CONCLUSIONS

The impact of concentrated colloidal suspension drops onto solid surfaces was studied by high-speed imaging, and compared with Newtonian drops of similar viscosity.

Experiments show that concentrated colloidal suspension drops do not exhibit large inertial deformations, which suggests that the impact induces dilatancy and jamming of colloidal particles, which prevent the drop deformation.

On glass substrates, at longer time scales one can observe capillary-driven spreading, where the spreading rate is about the same as that of Newtonian drops.

On PTFE substrates, capillary spreading cannot be observed, and the drop base diameter remains constant after impact. The base diameter value depends on the impact Weber number, which suggests that wetting plays a negligible role in comparison to the initial inertial deformation and the subsequent jamming of the colloidal suspension.

ACKNOWLEDGMENTS

The Authors thank A. Schofield for particle synthesis and L. Isa for permission to reproduce flow curves from his thesis.

REFERENCES

[1] M. Rein, Phenomena of liquid-drop impact on solid and liquid surfaces, Fluid Dynamics Research, vol. 12(2), pp. 61-93, 1993.

[2] R. Rioboo, C. Tropea and M. Marengo, Outcomes from a drop impact on solid surfaces, Atomization & Sprays, vol. 11, pp. 155-166, 2001.

[3] R. Rioboo, M. Marengo and C. Tropea, Time evolution of liquid drop impact onto solid, dry surfaces, Exp. Fluids, vol. 33, pp. 112-124, 2002.

[4] A. L. Yarin, Drop impact dynamics: Splashing, spreading, receding, bouncing, Annu. Rev. Fluid Mech., vol. 38, pp. 159–192, 2006.

[5] R. G. Larson, The Structure and Rheology of Complex Fluids, Oxford University Press, New York, 1999.

[6] G. Astarita, G. Marrucci, Principles of Non-Newtonian Fluid Mechanics, McGraw-Hill, New York, 1974.

[7] G. German, V. Bertola, Review of drop impact models and validation with high-viscosity Newtonian fluids, Atomization and Sprays, vol. 19, pp. 787-807, 2009.

[8] J. A. Lewis, Colloidal Processing of Ceramics, Journal of the American Ceramic Society, vol. 83, pp. 2341-2359, 2000.
[9] D. I. Wilson, S. L. Rough, Exploiting the curious characteristics of dense solid–liquid pastes, Chemical Engineering Science, vol. 61, pp. 4147-4154, 2006.
[10] M. D. Haw, Jamming, two-fluid behaviour and self-filtration in concentrated colloidal suspensions, Physical Review Letters, vol. 92, 185506, 2004.
[11] G. Petekidis, D. Vlassopoulos, P. N. Pusey, Yielding and flow of sheared colloidal glasses, J. Phys.: Condens. Matter, vol. 16, S3955, 2004.
[12] K. N. Pham, G. Petekidis, D. Vlassopoulos, S. U. Egelhaaf, P. N. Pusey, W. C. K. Poon, Yielding of colloidal glasses, Europhysics Letters, vol. 75, pp. 624-630, 2006.
[13] W. J. Frith, P. d'Haene, R. Buscall, J. MewisShear thickening in model suspensions of sterically stabilized particles, J. Rheol. 40, 531-548 (1996)
[14] P. Coussot, Rheophysics of pastes: a review of microscopic modeling approaches, Soft Matter, vol. 3, pp. 528-540, 2007.
[15] D. Psaltis, S.R. Quake, C. Yang, Developing optofluidic technology through the fusion of microfluidics and optics, Nature, vol. 442, pp. 381–386, 2006.
[16] M. E. Cates, M. D. Haw and C. B. Holmes, Dilatancy, jamming and the physics of granulation, J. Phys. Cond. Matt., vol. 17, S2517, 2005.
[17] L. Antl, J. W. Goodwin, R. D. Hill, R. H. Ottewill, S. M. Owens, S. Papworth, J. A. Waters, The preparation of poly(methyl-methacrylate) lattices in non-aqueous media, Colloids and Surfaces, vol. 17, pp. 67-78, 1986.
[18] B. A. de L. Costello, P. F. Luckham, Th. F. Tadros, Investigation of the interaction forces of polymer-coated surfaces using force balance, rheology, and osmotic pressure results, Langmuir, vol. 8, pp. 464-468, 1992.
[19] J. D. Bernal, The bakerian lecture, 1962: The structure of liquids, Proceedings of the Royal Society A, vol. 280, pp. 290-321, 1964.
[20] W. W. Wood, J. D. Jacobson, Preliminary results from a recalculation of the Monte Carlo equation of state of hard spheres, Journal of Chemical Physics, vol. 27, pp. 1207-1208, 1957.
[21] P. N. Pusey, W. van Megen, Phase behaviour of concentrated suspensions of nearly hard colloidal spheres, Nature, vol. 320, pp. 340-342, 1986.
[22] L. Isa, Capillary flow of dense colloidal suspensions, Ph.D. Thesis, University of Edinburgh, 2008.
[23] M. I. Smith, R. Besseling, M. E. Cates, V. Bertola, Dilatancy in the flow and fracture of stretched colloidal suspensions, Nature Communications, vol. 1, 114, 2010.
[24] G. German, V. Bertola, Formation of viscoplastic drops by capillary breakup, Physics of Fluids, vol. 22, 033101, 2010.
[25] L. H. Tanner, The spreading of silicone oil drops on horizontal surfaces, J. Phys. D: Appl. Phys. 12, pp. 1473, 1979.